

Place-it-R1: Unlocking Environment-aware Reasoning Potential of MLLM for Video Object Insertion

Bohai Gu^{1,2} Taiyi Wu² Dazhao Du¹ Jian Liu¹ Shuai Yang³
 Xiaotong Zhao² Alan Zhao² Song Guo^{1†}

¹HKUST ²Tencent Video ³Peking University

[†]Corresponding author

Abstract

Modern video editing techniques have achieved high visual fidelity when inserting video objects. However, they focus on optimizing visual fidelity rather than physical causality, leading to edits that are physically inconsistent with their environment. In this work, we present Place-it-R1, an end-to-end framework for video object insertion that unlocks the environment-aware reasoning potential of Multimodal Large Language Models (MLLMs). Our framework leverages the Chain-of-Thought (CoT) reasoning of MLLMs to orchestrate video diffusion, following a Think-then-Place paradigm. To bridge cognitive reasoning and generative execution, we introduce three key innovations: First, MLLM performs physical scene understanding and interaction reasoning, generating environment-aware chain-of-thought tokens and inferring valid insertion regions to explicitly guide the diffusion toward physically plausible insertion. Then, we introduce MLLM-guided Spatial Direct Preference Optimization (DPO), where diffusion outputs are fed back to the MLLM for scoring, enabling visual naturalness. During inference, the MLLM iteratively triggers refinement cycles and elicits adaptive adjustments from the diffusion model, forming a closed-loop that progressively enhances editing quality. Furthermore, we provide two user-selectable modes: a plausibility-oriented flexible mode that permits environment modifications (e.g., generating support structures) to enhance physical plausibility, and a fidelity-oriented standard mode that preserves scene integrity for maximum fidelity, offering users explicit control over the plausibility-fidelity trade-off. Extensive experiments demonstrate Place-it-R1 achieves physically-coherent video object insertion compared with state-of-the-art solutions and commercial models.

1. Introduction

Video object insertion is fundamental to video editing [1, 26, 37]. Given a reference object and a background video, users aim to obtain insertion results that align with their textual instructions. Although recent Diffusion Transformers (DiT)-based methods [13, 36, 38] achieve impressive pixel-level quality, their video object insertions often lack physical-level consistency with the environment, as they are fundamentally trained to optimize visual fidelity rather than physical causality. For example, as shown in the top of Fig. 1, when a user asks to place a mug on a still lake surface, current models like VACE [13] may fulfill this request by placing the cup directly on the water. However, this leads to physical implausibility, as they are unable to reason that ceramic mugs should sink instead of float on water. Beyond **physical plausibility**, the inserted objects should exhibit contextually appropriate scale and environmental reflections, like lighting and shadow, and we conclude this as **visual naturalness**. Meanwhile, as illustrated in the bottom part of Fig. 1, existing mask-based video insertion methods [13, 29] require users to specify object insertion regions in each frame as extra conditions for diffusion. In this ball-dropping scenario, users who want to simulate realistic physics are expected to accurately provide the trajectory of the ball’s free fall and subsequent movements, which is both tedious and technically demanding.

Although training large-scale diffusion models with extensive physics-oriented datasets could potentially mitigate these limitations, like commercial models Kling [14] and Pika [21], such an approach would incur substantial costs in both human annotation and computational resources. On the other hand, Multimodal Large Language Models [2] (MLLMs) have demonstrated remarkable capabilities in multimodal understanding. Recent works have integrated diffusion models with MLLMs to tackle more complex editing tasks [18, 32]. However, these approaches primarily exploit MLLMs merely as encoders for their representation capabilities, while overlooking an important aspect: MLLMs inherently possess physical commonsense knowledge that

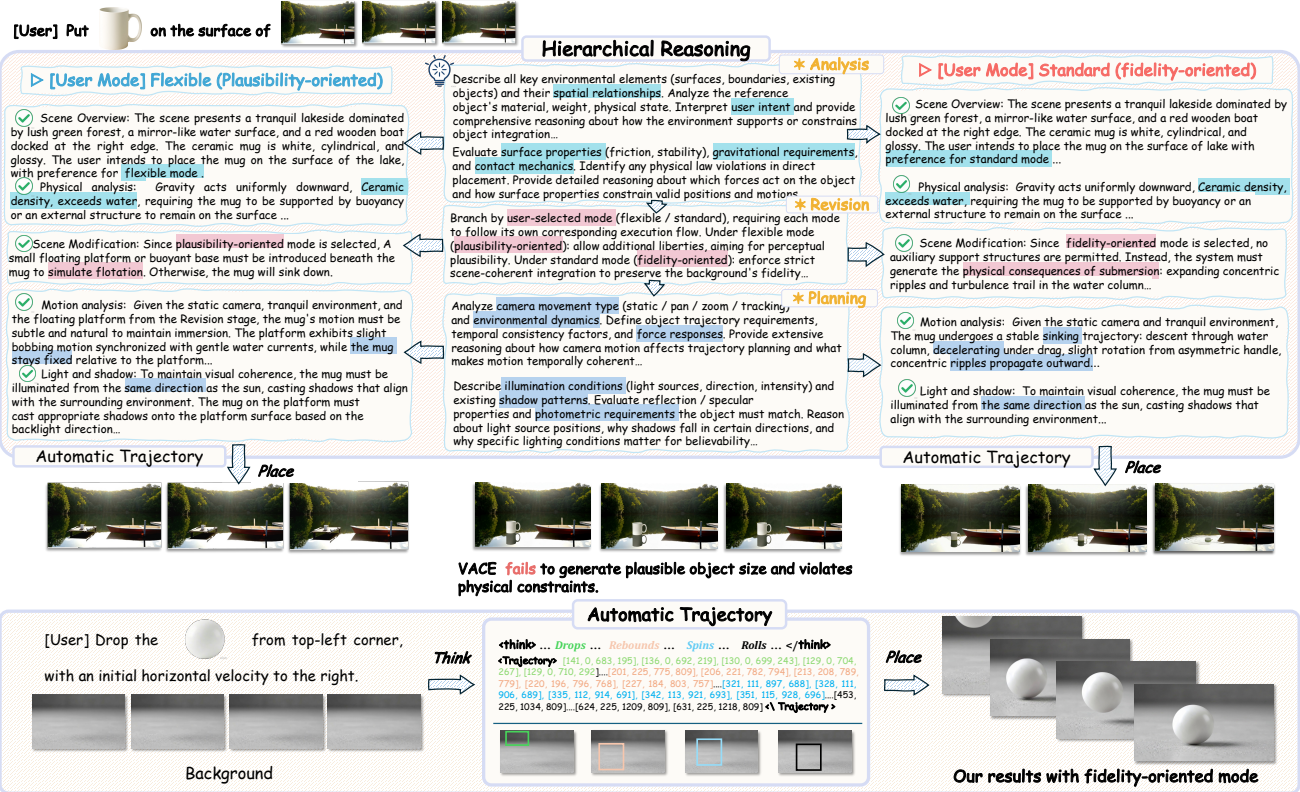


Figure 1. Place-it-R1 performs environment-aware video object insertion with automatic spatial planning, supporting two user-selectable modes. .

could be leveraged for physics-aware generation. To this end, we propose Place-it-R1, a MLLM-guided chain-of-thought reasoning pipeline built on DiTs for video object insertion. Our key insight is to leverage their Chain-of-Thought reasoning [33] to unlock their potential for environment-aware video object insertion without expensive retraining or burdensome user input.

As shown in the top-left of Fig. 2, Place-it-R1 leverages MLLMs as the **reasoning brain** to guide video diffusion models as the **executive hand**, following a Think-then-Place paradigm. Place-it-R1 has three core designs to help the brain and hands coordinate: Brain-to-Hand Command, Hand-to-Brain Feedback and Brain-Hand Co-refinement. First, MLLM brain conducts hierarchical reasoning, as illustrated in Fig. 1, generating environment-aware chain-of-thought tokens and inferring valid insertion regions to explicitly guide the diffusion model through an end-to-end pipeline. Specifically, this hierarchical reasoning follows a logical three-stage routine: (1) Detailed environment analysis to understand scene constraints, (2) Revision to reason about physics-driven object-background interactions, and (3) Generation of a detailed insertion plan to guide the diffusion process. Crucially, we observe that **achieving physical plausibility sometimes necessitates adaptive environment modifica-**

tions (e.g., generating a support structure for a mug on water). Thus, Place-it-R1 provides two user-selectable modes: a **flexible mode** that permits such environment adaptations when physical reasoning deems them necessary, and a **standard mode** that strictly maintains the original scene, which gives users explicit authority over the plausibility-fidelity trade-off. Second, to better bridge cognitive reasoning and generative execution, we also introduce MLLM-guided post-training, where the diffusion’s outputs are scored by MLLM to construct DPO preference pairs based on physical realism, we call this as hand-to-brain feedback. We further introduce Spatial DPO, a fine-grained optimization approach applied to preference pairs for superior visual naturalness. Finally, during inference, MLLM brain could continuously evaluates generation quality and triggers refinement cycles when needed, while the diffusion model responds adaptively. This establishes a closed-loop collaboration that progressively enhances overall editing quality. Briefly, We make three key contributions:

- To the best of our knowledge, we are the first to propose the Think-then-Place paradigm for video object insertion, unlocking the environment-aware reasoning potential of MLLM for physically plausible insertions.
- We present a systematic integration bridging the reasoning-

execution gap via MLLM-guided Spatial DPO and closed-loop co-refinement.

- Extensive experiments demonstrate Place-it-R1 achieves SoTA performance, even rivaling commercial models.

2. Related Work

2.1. Video Object Insertion

Video editing has witnessed rapid progress fueled by diffusion models [11, 27]. Early efforts explored training-free [8, 10] or one-shot tuning [34] strategies, while subsequent methods have pursued more structured designs [16, 19] to better realize temporal coherence. Recently, unified and scalable frameworks have emerged: AnyV2V [15] performs first-frame editing followed by I2V propagation; VACE [13] consolidates diverse editing tasks within a single system using Video Condition Units and context adapters; and UNIC [36] advances task unification by representing heterogeneous inputs as tokenized sequences, enabling in-context learning without task-specific adapters. Additionally, WAN [31], a foundational DiT for text-to-video generation, has established the groundwork for diverse editing applications. While these methods demonstrate impressive versatility across multiple editing tasks, they lack specialized mechanisms for video object insertion, particularly in modeling physically plausible object-environment interactions. video object insertion, which seeks to seamlessly integrate objects from reference images into target videos, has recently attracted growing attention [1, 26]. VideoAnydoor [29] enhances fidelity and motion control through a pixel warper, while DreamInsert [37] introduces a training-free paradigm for image-to-video object insertion. Moreover, Zhuang et al. [38] substitute the conventional U-Net [25] with a DiT architecture [20] that leverages 3D full attention for stronger temporal modeling. Despite these advances, most existing methods overlook real-world physical constraints, often resulting in unrealistic composites. By contrast, our approach incorporates Chain-of-Thought (CoT) [33] reasoning to pre-plan insertion, leading to more natural and physically consistent results.

2.2. Direct Preference Optimization

RLHF (Reinforcement Learning from Human Feedback) [3] has become a prevalent post-training paradigm for improving large language models [7] and diffusion models through human feedback [5]. A notable approach under this paradigm is Direct Preference Optimization (DPO) [24], which directly learns from pairs of preferred and non-preferred outputs, encouraging the model to assign higher likelihoods to human-preferred results. Inspired by DPO, several methods have extended its principles to diffusion models. For instance, Diffusion-DPO [30] introduces this framework to image generation, VideoDPO [17] adapts it to video diffu-

sion to enhance motion fidelity and temporal coherence, and DenseDPO [35] further improves scoring by segmenting sequences for finer-grained temporal alignment. Despite these advances, current efforts have predominantly focused on video generation, with video editing remaining largely unexplored, particularly the integration of custom subjects. Moreover, existing reward formulations are limited in their ability to assess realism. To address these gaps, we propose Spatial DPO, a variant that emphasizes the edited region and leverages MLLMs to provide realism-aware preference signals for optimization.

3. Place-it-R1 Framework

As illustrated in Fig. 2, our framework leverages MLLMs as the reasoning brain to guide video diffusion models as the executive hand. The overview of our framework can be divided into three stages: **(1) Brain-to-Hand Command:** We unlock the environment-aware reasoning potential of MLLMs for video object insertion and conduct thinking-aligned training (Sec. 3.1). **(2) Hand-to-Brain Feedback:** MLLM-guided physical preference dataset construction (Sec. 3.2) combined with Spatial DPO (Sec. 3.3); and **(3) Brain-Hand Co-Refinement** (Sec. 3.4): MLLM-guided refinement cycles.

3.1. Brain-to-Hand Command

Our framework employs Qwen-VL 2.5 [2] as the thinking brain to process multi-modal inputs including system prompts, user instructions, reference object images, and background video frames for video object insertion. As shown in Fig. 2, thinking proceeds in two steps: (1) hierarchical reasoning and (2) automatic trajectory generation.

3.1.1. Hierarchical Reasoning

As illustrated in Fig. 2, our hierarchical reasoning architecture comprises three stages: **(1) Analysis** provides comprehensive scene understanding, including background video context, inserted object properties, user instructions, and physical constraint modeling; **(2) Revision** branches by user-selected mode: under the flexible mode, the MLLM reasons about physics-driven object-background interactions and permits adaptive environment modifications (*e.g.*, generating support structures) to maximize physical plausibility; under the standard mode, the MLLM enforces strict scene integrity, preserving the original background while focusing solely on object-level adaptation; and **(3) Planning** generates detailed insertion guidance for the diffusion model, encompassing motion specifications for dynamics interaction and lighting/shadow analysis for photometric consistency.

3.1.2. Automatic Insertion Trajectory

The second step translates abstract interaction strategies into concrete physical coordinates. The MLLM leverages

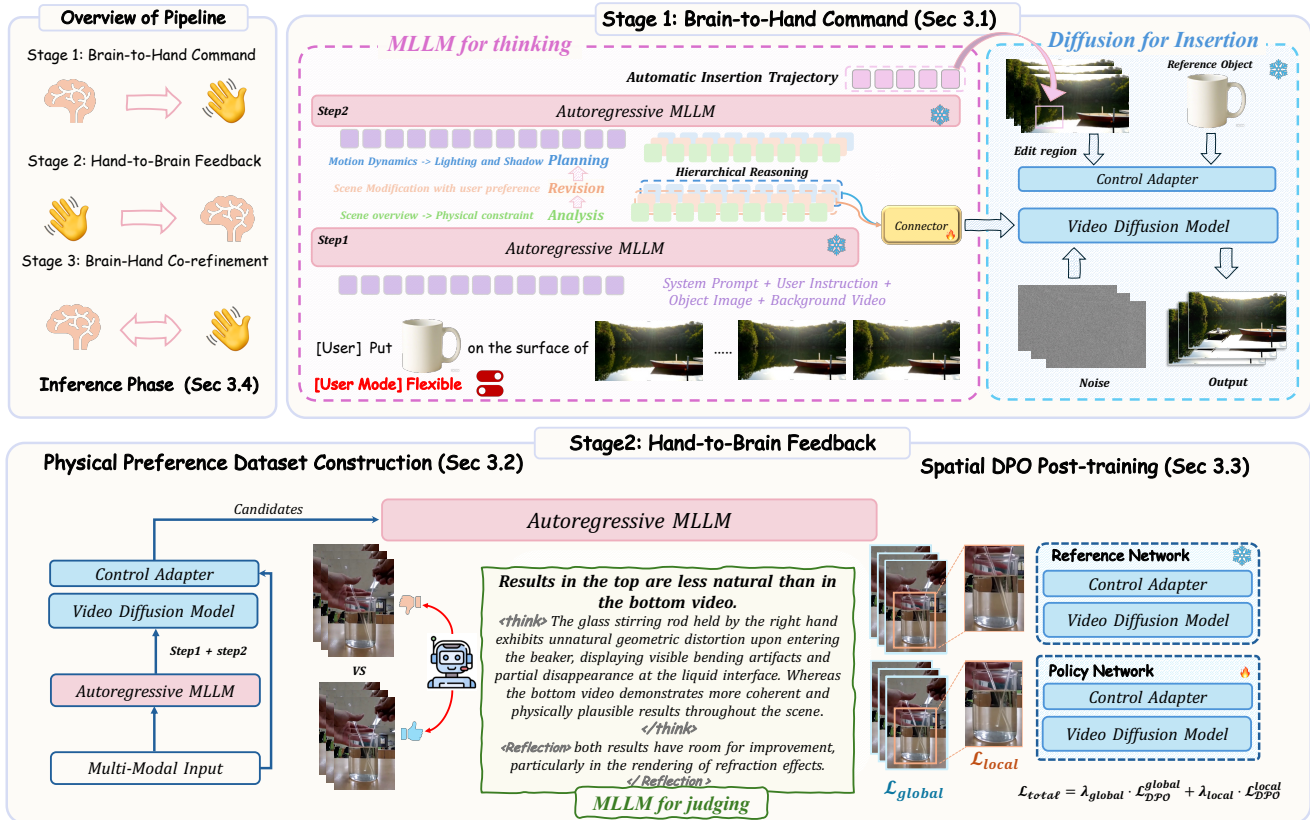


Figure 2. Overall pipeline of Place-it-R1, including details of Brain-to-Hand Command and Hand-to-Brain Feedback.

the generated hierarchical CoT tokens as additional context alongside the original multi-modal inputs, enabling spatially-aware reasoning. As shown in Fig. 2, this step determines *where* the object should be placed within each frame. The MLLM outputs precise bounding boxes $[x_1, y_1, x_2, y_2]$ that specify both the target object’s location and regions requiring environmental modifications (e.g., supporting surfaces or contact areas). These coordinates are subsequently converted into binary masks that provide pixel-level guidance for the diffusion generation process.

3.1.3. Thinking-aligned Training

Our generative pipeline builds upon the VACE [13] framework, extending Wan2.1 [31] for video object insertion. As illustrated in Fig. 2, we integrate reasoning output through two complementary conditioning pathways that work together to achieve physically plausible integration in an end-to-end manner. **(1) Semantic Conditioning Pathway.** This pathway translates high-level reasoning into generation guidance. We design a lightweight connector module that bridges the representation gap between the MLLM’s reasoning space and the diffusion model’s conditioning space. Specifically, the connector projects environment-aware interaction reasoning tokens, which are derived from the revision and planning

stages of our hierarchical reasoning, into the text embedding space used by Wan2.1. During training, the connector is optimized to preserve the semantic richness of reasoning outputs while producing effective conditioning signals for the diffusion model. This pathway captures *what* and *how* of object insertion, determining interaction types, physical behaviors, and photometric properties. **(2) Spatial Conditioning Pathway.** Complementing semantic guidance, the spatial pathway ensures precise localization of modifications by directly leveraging the binary masks generated from spatial grounding. While semantic conditioning governs the naturalness of interactions, spatial conditioning specifies *where* these interactions occur.

3.2. Physical Preference Dataset Construction

We employ Direct Preference Optimization (DPO) to enhance physical realism. The key challenge lies in collecting high-quality preference pairs for training. Given the absence of reliable automated metrics for quantifying physical plausibility, we leverage MLLM reasoning for preference assessment: a process we term *hand-to-brain feedback*. Specifically, given identical multi-modal inputs, we generate five insertion candidates using different random seeds following our Stage 1 pipeline. As illustrated in the lower

part of Fig. 2, we evaluate each candidate using MLLM in three dimensions: (i) object scale appropriateness, (ii) photometric consistency (lighting and shadow rendering), and (iii) physical interactions with the environment. Detailed system prompts and examples are provided in the supplementary material. To improve the reliability of MLLM-based evaluation, we implement two strategies. First, we provide the MLLM with the bounding boxes generated in Sec. 3.1.2, which is further highlighted as red boxes in the video, to focus the assessment on edited regions while minimizing background interference. Second, we employ a consensus ranking protocol: each candidate set is ranked twice with independently permuted orders, and preference pairs are only accepted when rankings remain consistent across both trials. This consensus mechanism effectively filters evaluation noise and ensures high-quality physical realism preference data pairs.

3.3. Spatial Direct Preference Optimization

Following Diffusion-DPO [30], given a winning sample v_w over a losing sample v_l , the standard DPO loss, which we denote as $\mathcal{L}_{DPO}^{global}$ since it operates uniformly over the full frame, is defined as:

$$\mathcal{L}_{DPO}^{global} = -\mathbb{E}_{(v_w, v_l)} [\log \sigma(\beta \Delta_{\theta, ref})], \quad (1)$$

where $\Delta_{\theta, ref} = (L_{\theta}^l - L_{\theta}^w) - (L_{\theta_{ref}}^l - L_{\theta_{ref}}^w)$ with $L = \|\epsilon(v^t, t) - \epsilon_{target}\|^2$ being the denoising loss, and the hyperparameter β controls the preference strength. The function $\sigma(\cdot)$ is the standard sigmoid function. As illustrated at the bottom of Fig. 2, we designate the pretrained diffusion from the first stage as the reference model θ_{ref} with frozen parameters, while a trainable policy model θ is initialized from θ_{ref} and fine-tuned to align with preferences dataset. A key observation is that standard Diffusion-DPO applies uniform optimization across the entire frame, yet physical plausibility violations, like contact artifacts and scale errors, are highly localized at the insertion region, making global-only optimization inefficient. To address this, we introduce Spatial DPO, our key insight is to focus on fine-grained optimization within the insertion regions defined by bounding boxes from our reasoning pipeline. We introduce a mask-weighted denoising loss, defined for a given binary spatial mask \mathcal{M} that identifies an insertion region:

$$L(v, \mathcal{M}) = \|(\epsilon(v^t, t) - \epsilon_{target}) \odot \mathcal{M}\|^2, \quad (2)$$

where \odot denotes the element-wise product. The local loss is then formulated by substituting the standard loss with this mask-weighted variant for both winning and losing samples:

$$\mathcal{L}_{DPO}^{local} = -\mathbb{E}_{(v_w, v_l, \mathcal{M})} [\log \sigma(\beta \Delta_{\theta, ref}^{local})], \quad (3)$$

where $\Delta_{\theta, ref}^{local}$ is computed using the masked loss $L(v, \mathcal{M})$. The proposed Spatial DPO specifically enhances critical

details where physical realism matters most, ensuring visually natural contact dynamics at the insertion boundaries, as demonstrated in our experimental evaluations.

Final Objective. The final DPO training objective combines both losses to balance local detail refinement and global coherence with hyperparameters λ_{global} and λ_{local} :

$$\mathcal{L}_{total} = \lambda_{global} \cdot \mathcal{L}_{DPO}^{global} + \lambda_{local} \cdot \mathcal{L}_{DPO}^{local}. \quad (4)$$

3.4. Brain-Hand Co-refinement

During inference, our MLLM iteratively triggers refinement cycles that elicit adaptive adjustments from the diffusion model, forming a closed-loop system that progressively enhances editing quality. After each generation pass, the MLLM performs a comprehensive post-evaluation in three critical dimensions: (i) object scale appropriateness, (ii) photometric consistency, and (iii) physical interactions with the environment as in Sec. 3.2. As illustrated in Fig. 3, this iterative refinement process systematically addresses multifaceted quality issues. The initial generation exhibits deficiencies in hand-object dynamics interactions. The MLLM’s diagnostic evaluation identifies these failure modes and automatically triggers corrective refinement by updating both the interaction chain-of-thought and spatial guidance. After the second generation improves interaction coherence, the MLLM detects other issues in scale consistency and lighting, prompting another refinement iteration. The cycle terminates only when the MLLM’s evaluation confirms both physical plausibility and visual coherence. This MLLM-driven post-evaluation paradigm validates that complex editing tasks benefit from iterative assessment and targeted correction rather than single-pass generation. While our system typically achieves convergence within 2-3 iterations for complex cases, we set the iteration count to 1 in our main experiments for computational efficiency and fair comparisons. The detailed refinement protocols are described in the supplementary material.

4. Experiments

4.1. Implementation Details

Place-it-R1 is built upon QwenVL2.5-7B and WAN 1.3B, and the control adapter is initialized from VACE 1.3B. The connector module, consisting of a two-layer MLP, trained with flow matching loss: $\mathcal{L}_{FM} = \mathbb{E}_{t, x_t} \|v_{\theta}(x_t, t, c) - u_t\|^2$ where v_{θ} is the predicted velocity and u_t is the target flow. We use AdamW (lr = 10^{-3} , bs = 2) for 500K iterations on 32 H20 GPUs, while keeping other components frozen. For DPO post-training, we fine-tune WAN and VACE using LoRA (rank 128) for 10K iterations with a batch size of 8. β is setting to 100, and λ_{global} , λ_{local} are setting to 0.5. Notably, Place-it-R1 supports flexible user interaction: users can directly specify editing regions, bypassing

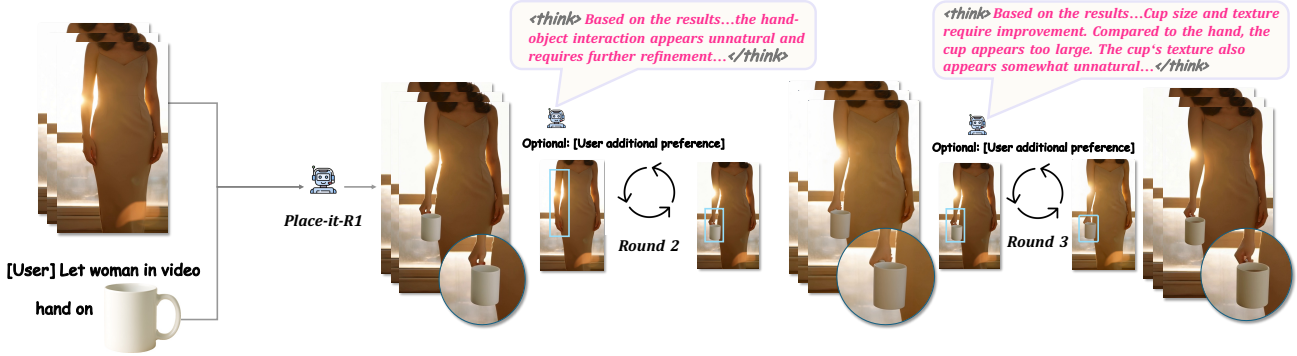


Figure 3. Brain-Hand Co-refinement mechanism progressively improves editing quality based on the MLLM post-evaluation.

the automatic region generation in Sec. 3.1.2. This flexibility is leveraged during training, where we use pre-masked videos from our dataset to eliminate Step 2 computation in Sec. 3.1.2, improve training efficiency. To conduct training in Stage 1 (Sec. 3.1) and 2 (Sec. 3.2), we construct a custom subject integration dataset. While synthetic trajectory generation using MLLMs presents an intuitive approach, it faces expensive manual verification and lacks ground truth validation. We therefore adopt a reverse-engineering approach leveraging real-world videos from two complementary categories: (i) human-object interaction videos (10,198 samples) capturing natural manipulation behaviors, and (ii) physics-demonstration videos (10,352 samples) showcasing physical phenomena including collisions, combustion, and gravitational dynamics. Data curation pipeline and details are provided in the supplementary material.

4.2. Comparison with State-of-the-Art Methods

4.2.1. Quantitative comparisons.

We conduct comprehensive quantitative evaluation on three benchmarks: (i) HumanSync (100 samples), a human-object interaction benchmark that provides accurate insertion regions. We compare VACE [13] on this benchmark by providing it with a simplified CoT as a prompt. (ii) FlexInsert (100 samples), which requires inserting objects into pure background videos, thus challenging the model to autonomously identify and generate reasonable insertion locations. We compare Place-it-R1 with VACE and AnyV2V [15] combined with Anydoor [9]. To make the comparison more convincing, instead of providing VACE with the same insertion regions used by our method, we supply it with insertion regions generated by MLLM without CoT tokens as conditional context (see Sec. 3.1.2). (iii) UNIC [36] benchmark (20 samples), which also provides no insertion regions. For this benchmark, we compare our method against the closed-source UNIC model and the commercial models Lucy-Edit pro [22], Pika [21] and Kling [14]. We evaluate across three dimensions: Identity Preservation (CLIP-I [23] and DINO-I [6]), Video Quality [12] (temporal smoothness

and aesthetics). Physical metrics are measured using the VideoPhY2 benchmark [4], which quantitatively assesses Physical Commonsense (PC) and Physical Rules (PR) adherence. We further introduce Gemini Pro [28] to evaluate Physical Plausibility (PP) of generated videos. As shown in Table 1, Place-it-R1 consistently achieves the best performance in physical realism metrics while demonstrating notable performance on video quality and identity metrics. Specifically, the PC [4] and PR [4] scores show substantial improvements over VACE (7.75%) and UNIC (9.52%). Notably, we conduct a systematically designed human evaluation to assess physical plausibility and video quality on the Flexinsert benchmark with 10 independent annotators who evaluated different tasks. Specifically, as shown in Fig. 7, the evaluation consists of two types: the top panel shows a three-way preference selection where annotators chose their most preferred method, while the bottom two panels present 1v1 comparisons between Place-it-R1 and each baseline method. Our results show Place-it-R1 significantly outperforms existing methods, improving performance in physical plausibility and visual quality.

4.2.2. Qualitative Comparisons.

We compare Place-it-R1 (flexible mode) with VACE [13], Kling [14] and pika [21]. Since UNIC is not open-source, we utilize their demos for comparisons in supplementary material. For a convincing comparison, we also provide mask-based method VACE with the simplified CoT and insertion regions generated by MLLM without CoT tokens as conditional context.

As demonstrated in Fig. 4, Place-it-R1 shows superior performance in video object insertion that are not only visually coherent but also physically plausible. **Top-Left** (Physics-based interactions): When tasked with placing a mug on a lake’s surface, baseline methods fail to adhere to basic physical laws, either placing the mug directly on the water or incorrectly on the boat at an unrealistic scale. In contrast, Place-it-R1 exhibits strong commonsense reasoning. It correctly infers the need for a support structure, generating a floating platform to realistically simulate flotation while

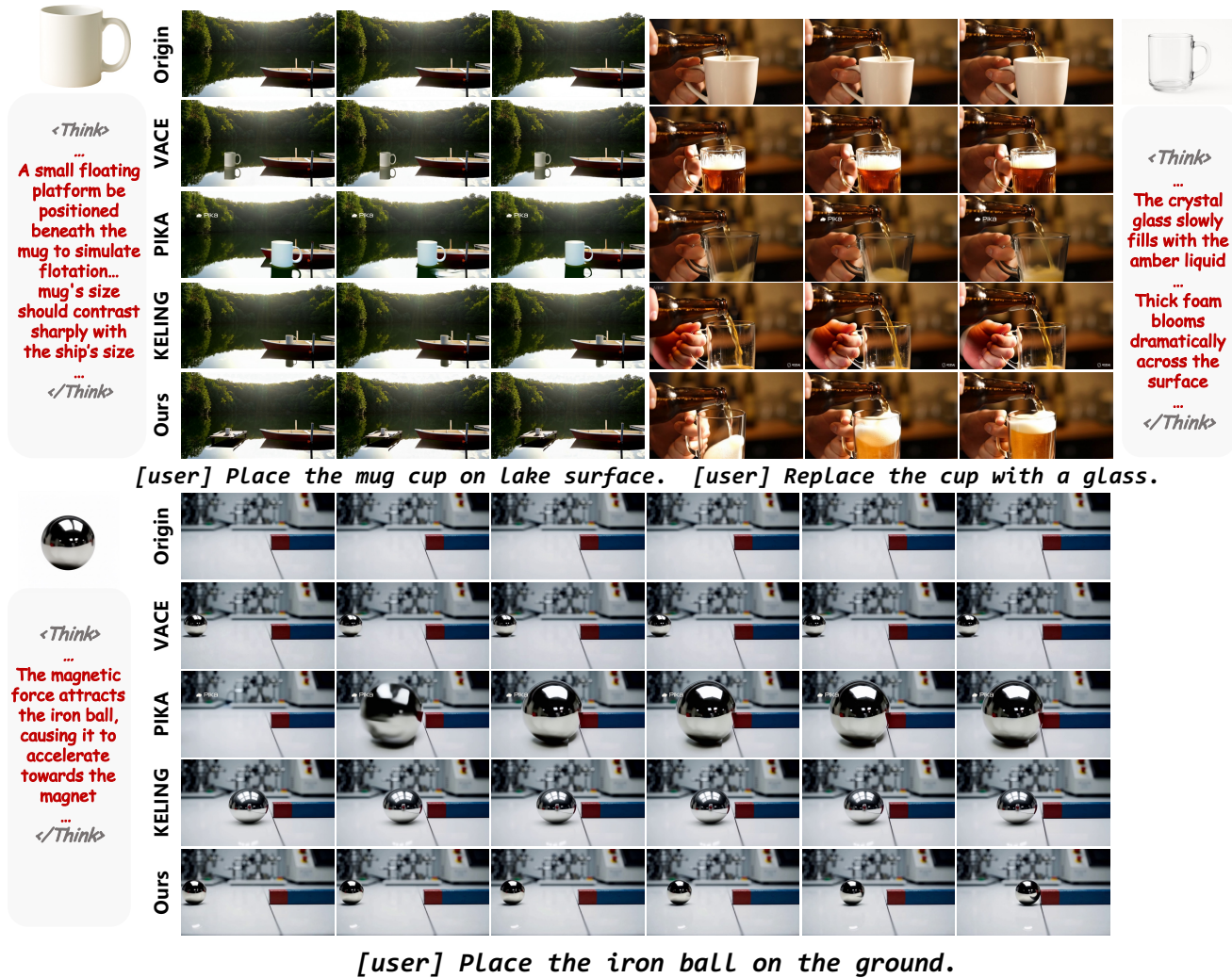


Figure 4. Qualitative Comparisons. The comparison illustrates Place-it-R1 achieves physically plausible environment-aware insertions.

ensuring the mug’s size is reasonable relative to the boat. **Top-Right (Fluid Dynamics):** In a challenging object-swap task where a cup is replaced with a glass during pouring beer, only our method successfully models the fluid dynamics. It realistically depicts the beer filling the glass and overflowing with authentic foam formation. Other methods fail to capture these dynamic properties, resulting in static or physically inconsistent outcomes. **Bottom (Implicit Force Reasoning):** The advantage of our MLLM-guided reasoning is most evident in the bottom scenario. Given the instruction to place an iron ball in an environment with a magnet, Place-it-R1 is the only method that correctly interprets the unseen magnetic force. It vividly renders the ball accelerating towards the magnet, demonstrating a deep understanding of the scene’s underlying physics. Competing methods fail to recognize this crucial context, generating a ball of incorrect size and with implausible motion. These results validate Place-it-R1’s

extraordinary capability in achieving both visual fidelity and physical plausibility in complex, dynamic scenarios.

4.3. Ablation Study

We conduct ablation studies under the flexible setting of Place-it-R1.

Does CoT improve insertion trajectory?

Without CoT tokens from hierarchical reasoning (Sec. 3.1.2), the MLLM generates insertion regions that lack physical-aware prior analysis, leading to overly simplistic or erroneous trajectories. As shown in Fig. 6, when placing a box on an operating treadmill, the MLLM without CoT fails to account for forward friction force, producing an insertion trajectory (second row) with minimal displacement. The fourth row Tab. 2 also shows overall metrics decline compared to the full version.

Can T5-based prompting replace reasoning tokens? As

Table 1. Quantitative comparisons among three benchmarks. PC: Physical Commonsense, PR: Physical Rule, PP: Physical Plausibility. UNIC benchmark includes many virtual animated characters as objects, thus precluding the use of PR.

Benchmark	Method	Identity		Video Quality		Physics		
		CLIP-I ↑	DINO-I ↑	Smooth. ↑	Aesth. ↑	PC ↑	PR ↑	PP ↑
UNIC	UNIC [36]	0.5980	0.2450	0.9610	0.5627	4.20	/	5.33
	Kling (commercial model) [14]	<u>0.6203</u>	0.2509	0.9540	0.5641	4.41	/	5.93
	PIKA (commercial model) [21]	0.6862	0.3752	0.9944	0.6151	4.34	/	6.11
	Lucy-edit pro (commercial model) [22]	0.6021	0.2629	0.9865	0.5693	4.28	/	5.79
	Place-it-R1(standard mode)	0.6043	<u>0.2897</u>	<u>0.9928</u>	0.5684	<u>4.53</u>	/	<u>6.21</u>
	Place-it-R1(flexible mode)	0.6040	0.2895	0.9919	<u>0.5787</u>	4.60	/	6.63
FlexInsert	AnyV2V [15] + Anydoor [9]	0.7853	0.3805	0.9853	0.4833	3.87	0.66	3.38
	VACE + Trajectory (w/o CoT)	0.7285	0.2541	<u>0.9913</u>	0.4920	4.03	0.67	5.21
	Place-it-R1(standard mode)	0.7941	<u>0.4917</u>	0.9918	<u>0.5294</u>	<u>4.13</u>	<u>0.78</u>	<u>7.28</u>
	Place-it-R1(flexible mode)	<u>0.7938</u>	0.4925	0.9906	0.5305	4.17	0.86	7.93
HumanSync	VACE [13]	0.7553	0.4210	0.9908	0.4952	4.12	<u>0.91</u>	6.21
	Place-it-R1(standard mode)	<u>0.7631</u>	<u>0.4497</u>	0.9929	<u>0.5283</u>	<u>4.33</u>	0.92	<u>6.58</u>
	Place-it-R1(flexible mode)	0.7632	0.4500	<u>0.9926</u>	0.5295	4.37	0.92	6.93

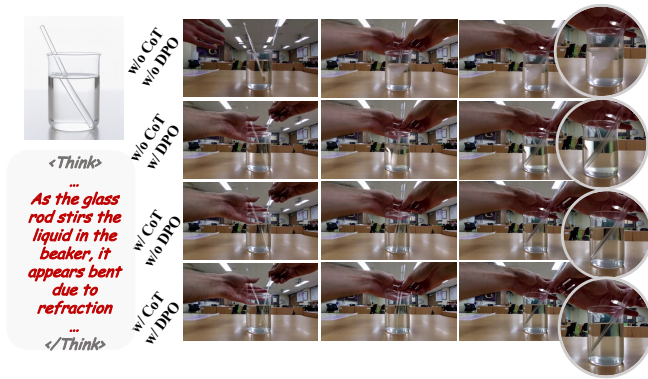


Figure 5. CoT and Spatial DPO work in synergy to enhance physical plausibility and visual naturalness, respectively.

shown in the third row of Tab. 2, we replaced the CoT token with plain text to validate its effectiveness. This change led to a drop across all metrics, which we attribute to two factors. First, the MLLM’s language space possesses a much richer representational capacity than standard text encoders T5. Second, our CoT token is a continuous representation that

Table 2. Ablation study on benchmark of FlexInsert.

Variant	Identity		Video Quality		Physics	
	CLIP-I ↑	DINO-I ↑	Smooth. ↑	Aesth. ↑	PC ↑	PR ↑
Place-it-R1 w / o CoT	0.7678	0.4489	0.9862	0.4989	3.92	0.67
Place-it-R1 w / o DPO	0.7721	0.4548	0.9891	0.4936	4.09	0.75
Place-it-R1 w CoT (Text)	0.7832	0.4492	0.9892	0.5102	4.02	0.69
Place-it-R1 w Trajectory (w / o CoT)	0.7305	0.3747	0.9923	0.5137	4.05	0.70
Place-it-R1	0.7938	0.4925	0.9906	0.5305	4.17	0.86

Table 3. Ablation study on parameters of Spatial DPO.

Superparameter	Identity		Video Quality		Physics	
	CLIP-I ↑	DINO-I ↑	Smooth. ↑	Aesth. ↑	PC ↑	PR ↑
$\lambda_{local} = 0.9, \lambda_{global} = 0.1$	0.7932	0.4832	0.9861	0.5254	4.06	0.69
$\lambda_{local} = 0.5, \lambda_{global} = 0.5$	0.7938	0.4925	0.9906	0.5305	4.17	0.86
$\lambda_{local} = 0.3, \lambda_{global} = 0.7$	0.7917	0.4713	0.9906	0.5265	4.15	0.79

Table 4. Inference cost and performance (HumanSync) of refinement iterations.

Step=5, CFG=5	Runtime(s) ↓	DINO-I ↑	Smooth. ↑	Aesth. ↑	PC ↑
VACE	15.15	0.421	0.9908	0.4952	4.12
Place-it-R1	18.07	0.450	0.9926	0.5295	4.37
Place-it-R1 with 1 iteration	38.06	0.455	0.9931	0.5315	4.46
Place-it-R1 with 2 iteration	60.13	0.457	0.9934	0.5327	4.53

preserves dense environmental context, unlike discrete text. This demonstrates that our end-to-end architecture, which directly utilizes this information-rich token, is essential for optimal performance.

Plausibility-fidelity trade-off. To quantify the plausibility-fidelity trade-off between the two modes, we evaluate on the FlexInsert benchmark, using Gemini Pro to assess scene fidelity, which measures the degree of background preservation relative to the original video. As shown in Fig. 8, the standard mode preserves higher scene fidelity by faithfully maintaining the original background, while the flexible mode achieves notably stronger physical plausibility by adaptively modifying the environment when physics demands it. They both offer complementary strengths along different axes, allowing users to freely select the appropriate mode based on their specific editing priorities.



Figure 6. Effect of CoT on insertion trajectory generation.

Key Contribution Ablation. As shown in Tab. 2, the first two rows demonstrate that variants without CoT tokens or without Spatial DPO training both exhibit performance degradation across all metrics. Beyond these quantitative results, Fig. 5 provides qualitative validation through a challenging human-interaction scenario. The task involves placing a beaker on a laboratory table with complex interaction.

The baseline (without CoT and DPO) produces severe artifacts including temporal flickering. DPO alone dramatically improves visual naturalness by eliminating boundary artifacts and producing smoother object motion but fails to achieve physically plausible interactions. CoT alone establishes physical plausibility but yields optically degraded refraction. The complete Place-it-R1 unifies both strengths, achieving physically accurate insertion with realistic fluid dynamics, correct refraction, and temporal coherence.

Parameters of Spatial DPO. As demonstrated in Tab. 3, we analyze the impact of Spatial DPO hyperparameters. When λ_{local} significantly exceeds λ_{global} (e.g., row 1: $\lambda_{local} = 0.9$, $\lambda_{global} = 0.1$), local details improve but insufficient global optimization causes background flickering, resulting

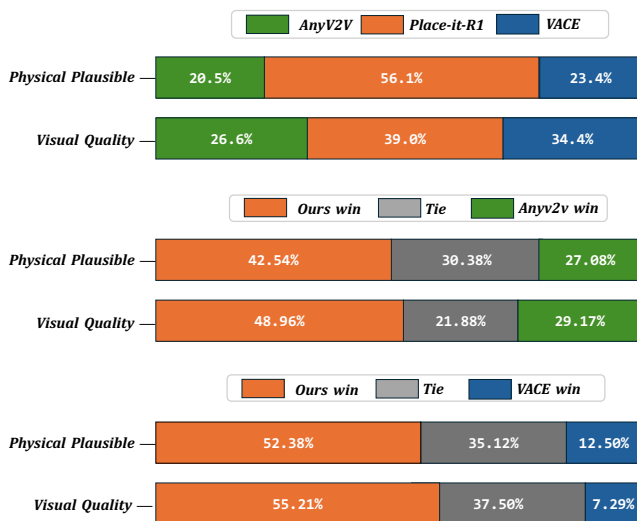


Figure 7. User study on benchmark of FlexInsert.

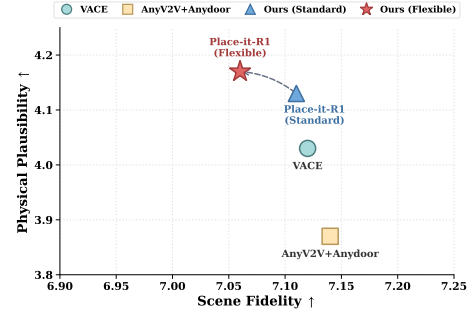


Figure 8. Plausibility-fidelity trade-off.

in a substantial decline in temporal smoothness. Conversely, balanced weights ($\lambda_{local} = 0.5$, $\lambda_{global} = 0.5$) achieve optimal performance across all metrics.

Iterative Refinement. We conduct inference experiments on HumanSync with single H800 (see Tab. 4). While it introduces additional latency for MLLM reasoning and refinement, the significant gains in performance represent a justifiable trade-off.

4.4. Discussion

Limitations The current framework relies on MLLM reasoning quality, which may occasionally produce suboptimal guidance for highly unusual or abstract editing requests. Additionally, as shown in Tab. 4, inference efficiency degrades as the number of refinement iterations increases, posing a practical challenge for latency-sensitive applications.

Future Direction. Beyond video editing, our framework suggests a broader perspective: MLLMs equipped with structured CoT reasoning can serve as lightweight world models that predict how objects interact with their environment. This capability opens promising directions for physics-aware video data synthesis, where Place-it-R1 could function as a controllable data generation engine to produce large-scale videos with physically grounded object-environment interactions, potentially benefiting downstream tasks such as embodied AI and robotics simulation.

5. Conclusion

We presented Place-it-R1, a novel framework that reformulates video object insertion from direct synthesis to a deliberate Think-then-Place paradigm. By introducing environment-aware MLLM-guided reasoning before generation, combined with Spatial DPO post-training and iterative corrective editing, our approach achieves both physical plausibility and visual naturalness in video editing. Furthermore, our dual-mode design provides users explicit control over the plausibility-fidelity trade-off. This environment-aware paradigm eliminates the need for expensive model retraining or manual trajectory specification, instead leveraging

MLLMs as brain whose physical commonsense guides generation. Extensive experiments confirm that Place-it-R1 outperforms state-of-the-art methods, particularly in scenarios requiring complex physical reasoning.

References

- [1] Chen Bai, Zeman Shao, Guoxiang Zhang, Di Liang, Jie Yang, Zhuorui Zhang, Yujian Guo, Chengzhang Zhong, Yiqiao Qiu, Zhendong Wang, et al. Anything in any scene: Photorealistic video object insertion. *arXiv preprint arXiv:2401.17509*, 2024. 1, 3
- [2] Shuai Bai, Keqin Chen, Xuejing Liu, Jialin Wang, Wenbin Ge, Sibao Song, Kai Dang, Peng Wang, Shijie Wang, Jun Tang, et al. Qwen2.5-vl technical report. *arXiv preprint arXiv:2502.13923*, 2025. 1, 3
- [3] Yuntao Bai, Andy Jones, Kamal Ndousse, Amanda Askell, Anna Chen, Nova DasSarma, Dawn Drain, Stanislav Fort, Deep Ganguli, Tom Henighan, et al. Training a helpful and harmless assistant with reinforcement learning from human feedback. *arXiv preprint arXiv:2204.05862*, 2022. 3
- [4] Hritik Bansal, Clark Peng, Yonatan Bitton, Roman Goldenberg, Aditya Grover, and Kai-Wei Chang. Videophy-2: A challenging action-centric physical commonsense evaluation in video generation. *arXiv preprint arXiv:2503.06800*, 2025. 6
- [5] Kevin Black, Michael Janner, Yilun Du, Ilya Kostrikov, and Sergey Levine. Training diffusion models with reinforcement learning. *arXiv preprint arXiv:2305.13301*, 2023. 3
- [6] Mathilde Caron, Hugo Touvron, Ishan Misra, Hervé Jégou, Julien Mairal, Piotr Bojanowski, and Armand Joulin. Emerging properties in self-supervised vision transformers. In *Proceedings of the IEEE/CVF international conference on computer vision*, pages 9650–9660, 2021. 6
- [7] Stephen Casper, Xander Davies, Claudia Shi, Thomas Krendl Gilbert, Jérémy Scheurer, Javier Rando, Rachel Freedman, Tomasz Korbak, David Lindner, Pedro Freire, et al. Open problems and fundamental limitations of reinforcement learning from human feedback. *arXiv preprint arXiv:2307.15217*, 2023. 3
- [8] Duygu Ceylan, Chun-Hao P Huang, and Niloy J Mitra. Pix2video: Video editing using image diffusion. In *Proceedings of the IEEE/CVF International Conference on Computer Vision*, pages 23206–23217, 2023. 3
- [9] Xi Chen, Lianghua Huang, Yu Liu, Yujun Shen, Deli Zhao, and Hengshuang Zhao. Anydoor: Zero-shot object-level image customization. In *Proceedings of the IEEE/CVF conference on computer vision and pattern recognition*, pages 6593–6602, 2024. 6, 8
- [10] Michal Geyer, Omer Bar-Tal, Shai Bagon, and Tali Dekel. Tokenflow: Consistent diffusion features for consistent video editing. In *The Twelfth International Conference on Learning Representations*, 2024. 3
- [11] Jonathan Ho, Ajay Jain, and Pieter Abbeel. Denoising diffusion probabilistic models. *Advances in neural information processing systems*, 33:6840–6851, 2020. 3
- [12] Ziqi Huang, Yanan He, Jiashuo Yu, Fan Zhang, Chenyang Si, Yuming Jiang, Yuanhan Zhang, Tianxing Wu, Qingyang Jin, Nattapol Chanpaisit, et al. Vbench: Comprehensive benchmark suite for video generative models. In *Proceedings of the IEEE/CVF Conference on Computer Vision and Pattern Recognition*, pages 21807–21818, 2024. 6
- [13] Zeyinzi Jiang, Zhen Han, Chaojie Mao, Jingfeng Zhang, Yulin Pan, and Yu Liu. Vace: All-in-one video creation and editing. *arXiv preprint arXiv:2503.07598*, 2025. 1, 3, 4, 6, 8
- [14] Keling. Image to video elements feature. <https://app.klingai.com/cn/multimodal-to-video/add-object/new>, 2025. Accessed: 2025-11-14. 1, 6, 8
- [15] Max Ku, Cong Wei, Weiming Ren, Harry Yang, and Wenhui Chen. Anyv2v: A tuning-free framework for any video-to-video editing tasks. *arXiv preprint arXiv:2403.14468*, 2024. 3, 6, 8
- [16] Jun Hao Liew, Hanshu Yan, Jianfeng Zhang, Zhongcong Xu, and Jiashi Feng. Magicedit: High-fidelity and temporally coherent video editing. *arXiv preprint arXiv:2308.14749*, 2023. 3
- [17] Runtao Liu, Haoyu Wu, Ziqiang Zheng, Chen Wei, Yingqing He, Renjie Pi, and Qifeng Chen. Videodpo: Omni-preference alignment for video diffusion generation. In *Proceedings of the Computer Vision and Pattern Recognition Conference*, pages 8009–8019, 2025. 3
- [18] Chen Min, Dawei Zhao, Liang Xiao, Yiming Nie, and Bin Dai. Uniworld: Autonomous driving pre-training via world models. *arXiv preprint arXiv:2308.07234*, 2023. 1
- [19] Chong Mou, Mingdeng Cao, Xintao Wang, Zhaoyang Zhang, Ying Shan, and Jian Zhang. Revideo: Remake a video with motion and content control. *Advances in Neural Information Processing Systems*, 37:18481–18505, 2024. 3
- [20] William Peebles and Saining Xie. Scalable diffusion models with transformers. In *Proceedings of the IEEE/CVF international conference on computer vision*, pages 4195–4205, 2023. 3
- [21] Pika. Pika additions, 2025. 1, 6, 8
- [22] Lucy pro. Lucy edit pro, 2025. 6, 8
- [23] Alec Radford, Jong Wook Kim, Chris Hallacy, Aditya Ramesh, Gabriel Goh, Sandhini Agarwal, Girish Sastry, Amanda Askell, Pamela Mishkin, Jack Clark, et al. Learning transferable visual models from natural language supervision. In *International conference on machine learning*, pages 8748–8763. PmLR, 2021. 6
- [24] Rafael Rafailov, Archit Sharma, Eric Mitchell, Christopher D Manning, Stefano Ermon, and Chelsea Finn. Direct preference optimization: Your language model is secretly a reward model. *Advances in neural information processing systems*, 36:53728–53741, 2023. 3
- [25] Olaf Ronneberger, Philipp Fischer, and Thomas Brox. U-net: Convolutional networks for biomedical image segmentation. In *International Conference on Medical image computing and computer-assisted intervention*, pages 234–241. Springer, 2015. 3
- [26] Nirat Saini, Navaneeth Bodla, Ashish Shrivastava, Avinash Ravichandran, Xiao Zhang, Abhinav Shrivastava, and Bharat Singh. Invi: Object insertion in videos using off-the-shelf diffusion models. *arXiv preprint arXiv:2407.10958*, 2024. 1, 3

- [27] Jiaming Song, Chenlin Meng, and Stefano Ermon. Denoising diffusion implicit models. In *International Conference on Learning Representations*, 2021. 3
- [28] Gemini Team, Rohan Anil, Sebastian Borgeaud, and Jean-Baptiste Alayrac. Gemini: A family of highly capable multi-modal models, 2025. 6
- [29] Yuanpeng Tu, Hao Luo, Xi Chen, Sihui Ji, Xiang Bai, and Hengshuang Zhao. Videoanydoor: High-fidelity video object insertion with precise motion control. In *Proceedings of the Special Interest Group on Computer Graphics and Interactive Techniques Conference Conference Papers*, pages 1–11, 2025. 1, 3
- [30] Bram Wallace, Meihua Dang, Rafael Rafailov, Linqi Zhou, Aaron Lou, Senthil Purushwalkam, Stefano Ermon, Caiming Xiong, Shikhar Arora, and Matteo Hessel. Diffusion model alignment using direct preference optimization. *arXiv preprint arXiv:2311.12908*, 2023. 3, 5
- [31] Team Wan, Ang Wang, Baole Ai, Bin Wen, Chaojie Mao, Chen-Wei Xie, Di Chen, Feiwu Yu, Haiming Zhao, Jianxiao Yang, et al. Wan: Open and advanced large-scale video generative models. *arXiv preprint arXiv:2503.20314*, 2025. 3, 4
- [32] Cong Wei, Quande Liu, Zixuan Ye, Qiulin Wang, Xintao Wang, Pengfei Wan, Kun Gai, and Wenhua Chen. Univideo: Unified understanding, generation, and editing for videos. *arXiv preprint arXiv:2510.08377*, 2025. 1
- [33] Jason Wei, Xuezhi Wang, Dale Schuurmans, Maarten Bosma, Fei Xia, Ed Chi, Quoc V Le, Denny Zhou, et al. Chain-of-thought prompting elicits reasoning in large language models. *Advances in neural information processing systems*, 35:24824–24837, 2022. 2, 3
- [34] Jay Zhangjie Wu, Yixiao Ge, Xintao Wang, Stan Weixian Lei, Yuchao Gu, Yufei Shi, Wynne Hsu, Ying Shan, Xiaohu Qie, and Mike Zheng Shou. Tune-a-video: One-shot tuning of image diffusion models for text-to-video generation. In *Proceedings of the IEEE/CVF international conference on computer vision*, pages 7623–7633, 2023. 3
- [35] Ziyi Wu, Anil Kag, Ivan Skorokhodov, Willi Menapace, Ashkan Mirzaei, Igor Gilitschenski, Sergey Tulyakov, and Aliaksandr Siarohin. Densdpo: Fine-grained temporal preference optimization for video diffusion models. *arXiv preprint arXiv:2506.03517*, 2025. 3
- [36] Zixuan Ye, Xuanhua He, Quande Liu, Qiulin Wang, Xintao Wang, Pengfei Wan, Di Zhang, Kun Gai, Qifeng Chen, and Wenhua Luo. Unic: Unified in-context video editing. *arXiv preprint arXiv:2506.04216*, 2025. 1, 3, 6, 8
- [37] Qi Zhao, Zhan Ma, and Pan Zhou. Dreaminsert: Zero-shot image-to-video object insertion from a single image. *arXiv preprint arXiv:2503.10342*, 2025. 1, 3
- [38] Shaobin Zhuang, Zhipeng Huang, Binxin Yang, Ying Zhang, Fangyikang Wang, Canmiao Fu, Chong Sun, Zheng-Jun Zha, Chen Li, and Yali Wang. Get in video: Add anything you want to the video. *arXiv preprint arXiv:2503.06268*, 2025. 1, 3